Article

Luminescent $NaYF_4$:Yb,Er Upconversion Nanocrystal Colloids: Towards Controlled Synthesis and Near-Infrared Optical Response†

Hau V. Duong,[a,b] Quy-Tung Truong,[b] Thai-Hoa Tran,[b**] and Thanh-Dinh Nguyen[c*]

[a]Department of Chemistry, Hue University of Agriculture and Forestry, Hue 84054, Vietnam
[b]Department of Chemistry, College of Sciences, Hue University, Hue 84054, Vietnam
[c]Department of Chemistry, University of British Columbia, 2036 Main Mall, Vancouver, BC, V6T 1Z1, Canada

*Corresponding Author: Dr. T.D. Nguyen, Email: ntdinhc@chem.ubc.ca
**Co-corresponding Author: Prof. Dr. T.H. Tran, Email: trthaihoa@yahoo.com

†This article has been accepted for publication and undergone full peer review but has not been through the copyediting, typesetting, pagination and proofreading process, which may lead to differences between this version and the Version of Record. Please cite this article as doi: [10.1002/cjce.22851]

Additional Supporting Information may be found in the online version of this article.

Received 2 October 2016; Revised 10 December 2016; Accepted 13 December 2016
The Canadian Journal of Chemical Engineering

DOI 10.1002/cjce.22851

Abstract: Lanthanide-doped upconversion nanocrystals are an emerging class of near-IR-sensitive luminescent nanomaterials that have aroused widespread interest in the investigation of their unique optical properties for sensing, biomedical, and energy applications. In this work, we have hydrothermally prepared $NaYF_4$:Yb,Er upconversion nanocrystals that can respond with brilliant photoluminescence to near-infrared laser light. The structural phase of the $NaYF_4$:Yb,Er upconversion nanocrystals can be controlled by extending the hydrothermal reaction to visibly tune their emission intensity. The highly photoluminescent $NaYF_4$:Yb,Er colloidal nanocrystals are subsequently assembled in host matrices of hard substrates and polymethyl methacrylate plastics by colloidal solution solidification to fabricate optical display components that may be useful as a potential alternative for fingerprint identification and encryption.

Keywords: upconversion nanomaterials, photoluminescence, photon energy transfer, optical plastics, self-assembly

INTRODUCTION

Photoluminescent materials have attracted much attention in many research fields ranging from biochemical sensing to energy conversion and storage.[1, 2] Luminescent materials, commonly called phosphors, typically undergo external energy excitation to emit light across a broad spectrum from ultraviolet to infrared.[3] Unique properties of electron transfer and optical response make them useful as light emissive units for developing practical applications in optical technology. Visible luminescence behaviour can be observed not only in the man-made nanomaterials by chemical and physical syntheses, but also appears in several specific species existing in nature.[4] Light-emitting structures of semiconductor quantum dots, metal complexes, and organic dyes are the most popular examples of artificial luminescent materials,[5, 6] while some fascinating creatures such as fireflies, jellyfish, and squid are widely known as optically active bio-species.[7]

Upconversion (UC) is a sequential absorption process of multiple photons of near infrared (NIR) light to emit brilliant luminescence tunable over the entire visible spectrum.[8] The phenomenal consequence of the luminescence appearance is that low energy light can be converted to high energy light. This photon UC process is known as an anti-Stokes type emission that is opposite to the down-conversion process of narrow band-gap semiconductors such as CdS and CdSe.[9] Unlike bioluminescence, UC emission mostly does not appear in nature since the UC process was early proposed by Bloembergen in the 1960s.[10] Lanthanide (Ln)-based UC nanomaterials are an optically active component for promising applications in infrared detection, bio-labels, biosensors, and solar cells, owing to the versatile chemical properties of the lanthanide-ion 4f electronic configuration.[11, 12] Among different types of the Ln-based UC materials,[13] sodium yttrium fluoride ($NaYF_4$) is an ideal host material for the incorporation of luminescent lanthanide (e.g. Yb, Er) ions to generate an optically active component. The Ln-doped $NaYF_4$ UC nanomaterial has been widely known to be a promising luminescent candidate for efficient photon upconversion of near infrared to visible radiation in a heterostructure caused by dopant-host interactions.[14] Ln-doped $NaYF_4$ generally comprises inorganic host, sensitizer, and activator, in which the sensitizer and activator are Ln ionic dopants homogeneously distributed in the $NaYF_4$ host lattice. Uniform co-doping of luminescent lanthanides into a $NaYF_4$ insulating matrix at nanoscale is thus a crucial factor to obtain homogeneous UC heterostructures that can respond with high-intensity photoluminescence to near-infrared excitation light.[15-17]

The scientific community has been devoted many wet-chemical synthetic methods such as hydro/solvothermalysis, thermal decomposition, microemulsion, and thermo-ultrasonication for controlled growth of Ln-doped $NaYF_4$ UC nanoparticles.[18-23] It is worth noting that the hydrothermal reaction is an effective pathway to synthesize highly luminescent Ln-doped $NaYF_4$

UC nanocrystals with well-defined shapes because of the facile incorporation of Ln ionic dopants into a $NaYF_4$ host lattice.[24, 25] Since structural diversity of the man-made UC materials is available to academia, the major goal of this implication is to push them beyond to explore their potential applications in the future.[26-28] Of particular note, high photon efficiency, low phototoxicity, and physicochemical stability lead the luminescent Ln-doped $NaYF_4$ UC nanomaterials possible to be optically active components for the development of colourful technology in fingerprint identification and encryption.[29, 30] It can also be interesting to design near infrared optical objects for anti-counterfeit document protection by integrating Ln-doped $NaYF_4$ UC nanoparticles into polymeric plastics.[31]

Herein, we aim to provide the controlled growth of chemically synthesized $NaYF_4$:Yb,Er UC nanocrystals in aqueous media. Stabilized $NaYF_4$:Yb,Er UC nanoparticle colloids with brilliant luminescence were used as an optically active guest to incorporate into host matrices of hard substrates and polymeric films to fabricate near infrared sensitized objects, presenting optical applications for colourful visualization.

EXPERIMENTAL

Chemicals

Yttrium nitrate hexahydrate ($Y(NO_3)_3.6H_2O$, ≥99.8 %), ytterbium nitrate pentahydrate ($Yb(NO_3)_3.5H_2O$, 99.9 %), erbium nitrate pentahydrate ($Er(NO_3)_3.5H_2O$, ≥99.9 %), ammonium fluoride (NH_4F, 99.99 %), sodium nitrate ($NaNO_3$, 98 %), methyl methacrylate (MMA, 99 %), 2,2-diethoxyacetophenone (98 %), oleic acid (OA, 90 %), ethylene glycol (EG, 99.8 %), and ethanol were received from Sigma-Aldrich and used as standard suppliers.

Materials Synthesis

Preparation of near-IR-sensitive $NaYF_4$:Yb,Er upconversion nanocrystals

149.3 mg $Y(NO_3)_3.6H_2O$, 449.0 mg $Yb(NO_3)_3.5H_2O$, and 45.0 mg $Er(NO_3)_3.5H_2O$ were dissolved in a mixture of 20 mL ethylene glycol and 20 mL ethanol under vigorous stirring at 60 °C to form a homogeneous aqueous solution. Another solution containing 332.0 mg $NaNO_3$, 144.3 mg NH_4F, 2 mL water, 20 mL ethanol, and 20 mL ethylene glycol was added dropwise to the above solution under stirring at 60 °C for 1 h to form a homogeneous aqueous mixture. The resulting mixture was transferred into a Teflon-lined autoclave with an internal volume of 200 mL, sealed, and heated to 180 °C in an oven. After heating for the desired reaction time, the bomb was naturally cooled to room temperature at 25 °C. The reaction mixture was diluted with ethanol and centrifuged to collect

white product colloids. For synthetic experiments of morphological and structural control, pure ethanol (40 mL) and ethanol-ethylene glycol-oleic acid (20:10:10 mL) were used as a reaction solvent, while keeping other reaction parameters unchanged. The hydrothermally reaction systems were also conducted by varying the reaction temperature and time. These products were assembled with hard surfaces of different substrates including lamellar woods, cloth fabrics, and polystyrene plastics for investigating the optical response of the resulting objects under near-IR laser excitation.

Preparation of $NaYF_4$:Yb,Er/PMMA plastic films

Near-IR-emitting plastic films were prepared by mixing 12 mL of toluene solution containing 5 mL methyl methacrylate and 80 μL 2,2-diethoxyacetophenone photoinitiator with 2 mL oleic acid/ethylene glycol-capped $NaYF_4$:Yb,Er nanocolloid toluene dispersion (0.02 g/g, 2 wt%) under stirring for 30 min at 25 °C to form a homogeneous mixed dispersion. The resulting mixture was poured into a 60 mm diameter glass Petri dish. During solvent evaporation at ambient conditions for at least 24 h, the reaction mixture was exposed to UV light (from an 8 W, 300 nm UV light source) to polymerize methyl methacrylate encapsulated around oleic acid/ethylene glycol-stabilized $NaYF_4$:Yb,Er nanoparticles, producing $NaYF_4$:Yb,Er/polymethyl methacrylate (PMMA) composite films.

Structural Characterization

Transmission electron microscopy (TEM) images of the samples were recorded on a JEOL 1010 electron microscope. A drop (~0.1 mL) of the colloidal nanoparticle solution was placed onto a carbon-coated copper grid and then dried at ambient conditions. Powder X-ray diffraction (PXRD) patterns of the samples were recorded on D8 advance X-ray diffractometer. Energy-dispersive X-ray (EDX) spectroscopy and EDX elemental mapping were collected using a Hitachi S2300 scanning electron microscope. Thermogravimetric analyses (TGA) of the samples (~1.0 mg) were conducted at a heating rate of 10 °C·min^{-1} under air to 850 °C using a PerkinElmer Pyris 6 thermogravimetric analyzer. Infrared spectra were obtained on neat samples using a Nicolet 4700 FT-IR. Room-temperature UC photoluminescence spectroscopy was obtained on a Hitachi F-4500 fluorimeter using a 800 mW lamp as a source with an excitation wavelength of 980 nm. Two-photon laser-scanning microscopy and lifetime decay were performed on a Zen LSM 510 Laser Module and a Tektronix DPO 4104 digital phosphor oscilloscope, respectively. The confocal laser scanning luminescent images obtained were analyzed using Zen software. Luminescence lifetime

decay curves recorded were fit with a single exponential model using a Single Photon Counter software.

RESULTS AND DISCUSSION

Our attempt in this work has investigated the controlled design of chemically synthesized $NaYF_4$:Yb,Er UC nanocrystals for fabricating objects with near infrared optical response. Precursor/capping agent aqueous mixtures underwent hydrothermal reaction to generate sized and shaped UC nanocrystalline colloids with tunable optical properties. Luminescent $NaYF_4$:Yb,Er UC nanocrystals were prepared by hydrothermal reaction of lanthanide nitrates and ammonium fluoride in an aqueous solution. White product colloids can be obtained from the hydrothermal reaction mixtures after ethanol washing and centrifugation. We have systematically tailored the influence of morphological and structural features of UC nanoparticles on different synthesis media and reaction conditions. Sequential integration involves the use of the as-made UC nanoparticles as an optical guest to incorporate within a matrix substrate, obtaining near infrared light-sensitive functional components potentially useful for advanced optical technologies.

The vast majority of nanomaterials research has focused on developing new synthetic approaches to Ln-doped $NaYF_4$ UC nanoparticles. Among them, the capping agent-assisted hydrothermal preparation of $NaYF_4$:Yb,Er nanoparticles has been realized as a facile method to control their shape and structural phase from past studies. As far as we know, the notable literatures of the polyol-mediated synthesis reported by Xu et al.[32] and the oleic acid-assisted two-phase hydrothermal synthesis reported by Zhang et al.[33] towards Ln-doped $NaYF_4$ nanomaterials have been considered as elegant examples to investigate their intriguing structural and optical properties. We generally note that the Ln-doped $NaYF_4$ UC materials undergo the growth confinement by polyol process to have small particle sizes while the anisotropic selective growth of the particles oriented by oleic acid capping agents results in well-defined crystalline structures. In this work, we have used these well-known synthetic methods with minor modifications to prepare $NaYF_4$:Yb,Er colloidal nanocrystals for investigating their structural, optical, and assembled features. In a typical synthesis, different synthesis media including ethanol (EtOH), ethanol-ethylene glycol (EtOH-EG), and ethanol-ethylene glycol-oleic acid (EtOH-EG-OA) were used in the hydrothermal reaction system to determine structural characteristics of UC nanoparticles. Powder X-ray diffraction patterns (PXRD) of these resulting samples are presented in Figure 1a. PXRD analyses confirm all diffraction peaks characteristic of a sodium rare-earth fluoride-type structure in all these samples obtained from different reaction media.[34] Diffraction diagrams exhibit strong and sharp peaks

resulting from a high degree of crystallinity of the as-prepared materials. Diffraction peaks of Ln ionic dopants (Er^{3+} and Yb^{3+}) or their derivatives cannot be detectable to prove a homogeneous incorporation of the optically active Ln dopants into the $NaYF_4$ host lattice. However, the variation of the components of structural phase in these samples can be distinguishable. The samples prepared in the mixtures of ethanol-ethylene glycol and ethanol-ethylene glycol-oleic acid both exhibit two polymorphic forms of major hexagonal β-phase and minor cubic α-phase. Conversely, a cubic α-phase was formed predominantly in the sample prepared in ethanol. These suggest that the nanocrystalline structure of the as-prepared $NaYF_4$:Yb,Er samples is highly dependent on steric effects of the stabilizers of ethylene glycol and oleic acid in the reaction media induced by changeable solvent-capping agent constituents.

The morphologies of the $NaYF_4$:Yb,Er nanocrystal samples prepared in different reaction media were observed with transmission electron microscopy (TEM) (Figures 1b–d). Electron microscope observation shows that the samples prepared in ethanol are spherical nanoparticles with a size range of 60–80 nm. The samples prepared in ethanol-ethylene glycol are roughly surfaced nanoparticles with a much smaller size of ~20 nm. The presence of oleic acid as a capping agent in ethanol-ethylene glycol led to stronger anisotropic growth of particles up to ~40–60 nm × 160–200 nm-sized nanorods along with some particle aggregates. These results verify that the morphology and crystalline phase of the $NaYF_4$:Yb,Er nanoparticles are highly sensitive to the reaction media so that their structural features can be tunable by using different capping agents/solvents while other reaction parameters the same.

The average particle size of the $NaYF_4$:Yb,Er nanoparticles hydrothermally prepared at 180 °C in ethanol-ethylene glycol estimated from the broadening (100) peaks using the Debye-Scherrer equation is about 25 nm, consistent with that observed by TEM image in Figure 1c. Energy-dispersive X-ray (EDX) analyses (Figures 1e and S1) reveal the presence of the main elements of Na, Y, F, Yb, Er in the UC nanoparticles hydrothermally prepared in ethanol-ethylene glycol at 180 °C, indicating the existence of a $NaYF_4$:Yb,Er structure formed by simultaneously doping Yb^{3+} and Er^{3+} ions into a $NaYF_4$ host lattice. These results prove that the hydrothermal synthesis effectively afforded the highly crystalline $NaYF_4$:Yb,Er nanoparticles. The TGA curve (Figure 1f) of the as-made $NaYF_4$:Yb,Er nanocrystals prepared in ethanol-ethylene glycol-oleic acid shows the decomposition of the organic stabilizers of ethylene glycol/oleic acid (~0.27 g/g, 27 wt%) adsorbed on the product at ~200–500 °C and a mass decrease of ~0.035 g/g (3.5 wt%) above 600 °C assigned to the oxidation of $NaYF_4$:Yb,Er. This confirmed these as-made products were surface-capped by ethylene glycol and oleic acid molecules.

We investigated structural phase transition of $NaYF_4$:Yb,Er nanocrystals by varying the reaction temperature, while keeping the remaining parameters unchanged. PXRD analyses (Figure 2a) confirm a binary mixture of major hexagonal *β*-phase and minor cubic *α*-phase in the $NaYF_4$:Yb,Er nanocrystal samples hydrothermally prepared in ethanol-ethylene glycol at 160, 180, and 200 °C, respectively. No trace of diffraction peaks corresponding to other phases or impurities can be detectable. Also, the crystalline phase of the $NaYF_4$:Yb,Er nanoparticles prepared in ethanol-ethylene glycol was controlled at different reaction times (12, 18, 36 h). PXRD patterns (Figure 2b) of these variable time-prepared samples show cubic *α*-to-hexagonal *β*-phase transition. We found that this structural phase transition takes approximately 36 h to entirely fulfill a pure β-hexagonal $NaYF_4$:Yb,Er crystalline structure. TEM images of these samples reveal that they are ~40 nm-sized particle aggregates formed in the early stages of hydrothermal reaction (~12 h) that grew up into spherical-like nanocrystals with larger particle sizes (15–20 nm) by extending the hydrothermal reaction time to 36 h (Figures 2c–e). These reveal a structural transition of the $NaYF_4$:Yb,Er nanocrystals from metastable cubic *α*-phase to thermodynamically stable hexagonal *β*-phase upon extended heating, which was also reported in the literature.[18, 35, 36]

The aqueous dispersions of the stabilized $NaYF_4$:Yb,Er nanoparticle colloids prepared in ethanol-ethylene glycol show strong photoluminescence under 980 nm laser excitation (Figure 3a). Drying the colloidal aqueous dispersion at room temperature afforded ethylene glycol-stabilized $NaYF_4$:Yb,Er UC nanosphere white solids that retain the brilliant green emission (Figure 3b) that is analogous to previously reported results.[37] It is reasonable to realize the surface properties of the UC nanospheres to be passivated by ethylene glycol to result in a negligible quenching effect of the UC luminescence. Optical properties of the as-prepared $NaYF_4$:Yb,Er UC nanocrystal samples were analyzed quantitatively. All the samples prepared using the different reaction conditions mostly respond well to UC luminescent spectroscopy. These samples exhibit emission peaks at the same wavelength position with tunable intensity. One of the representative samples of ethylene glycol-stabilized $NaYF_4$:Yb,Er UC nanocrystals hydrothermally prepared in ethanol-ethylene glycol was characterized in expression of its near-IR optical sensitivity by luminescent spectroscopy and lifetime decay. UC luminescence spectra (Figure 3c) of the ethylene glycol-stabilized UC nanoparticles under 980 nm laser excitation show three emission peaks at 525.0, 541.5, and 655.5 nm, which are assigned to the $^4H_{11/2}$–$^4I_{15/2}$ (green), $^4S_{3/2}$–$^4I_{15/2}$ (green), and $^4F_{9/2}$–$^4I_{15/2}$ (red) UC transitions, respectively, of the Er^{3+} ion dopants.[33] We also examined the reaction temperature-dependent optical properties of the as-made $NaYF_4$:Yb,Er upconversion nanocrystals with the goal of keeping other synthetic conditions unchanged. The optical spectroscopy shows that the materials exhibit enhanced emission intensity and their peak positions were preserved intact upon extended heating from 160 °C to 200 °C (Figure 3c). This spectral analysis is in accordance with variable

emission intensity of the different reaction temperature-synthesized $NaYF_4$:Yb,Er nanoparticle samples visibly observed by the naked eye. We also observed visibly the tunable intensity of photoluminescence in the $NaYF_4$:Yb,Er nanocrystal samples hydrothermally prepared using the variable lanthanide ratios (Figure S3). Note that the most promising UC luminescent nanomaterial is the hexagonal $NaYF_4$ phase because of its unusually high UC quantum yield. These results, combined with structural phase transition previously analyzed by X-ray diffraction, provide proof that the strong emission can be associated with the dominant hexagonal β-phase and the high degree of crystallinity in these as-made $NaYF_4$:Yb,Er nanomaterials.

UC luminescent lifetime decay of the ethylene glycol-stabilized UC nanoparticles dispersed in water was measured at 980 nm laser excitation and fit well to a single exponential function. Lifetime decay curves of Er^{3+} dopant emission at 525.0 nm, 541.5 nm, and 655.5 nm were as long as ~70, ~70, and ~120 μs ascribed to the $^4H_{11/2}$–$^4I_{15/2}$, $^4S_{3/2}$–$^4I_{15/2}$, and $^4F_{9/2}$–$^4I_{15/2}$ transitions, respectively (Figure 3e).[38, 39] The decay time of the red emission is longer than the green emission and these values are comparable with those of the UC nanoparticles reported by Liu et al.[36] It can be explained that the photon conversion of near infrared light to visible light over a $NaYF_4$ host lattice co-doped with Yb^{3+} and Er^{3+} guest is caused by two-photon energy transfer process from Yb^{3+} to Er^{3+} dopants. Under 980 nm laser irradiation, the electron of Yb^{3+} is first excited from $^2F_{7/2}$ to $^2F_{5/2}$ level in the $NaYF_4$:Yb,Er nanocrystals. An initial photon energy transferred from Yb^{3+} in $^2F_{5/2}$ state to Er^{3+} populates the $^4I_{11/2}$ level of Er^{3+}. A second photon energy transferred by the adjacent Yb^{3+} subsequently populates the $^4F_{7/2}$ level of Er^{3+}. These excited energies of Er^{3+} lie in the visible region, which can relax non-radiatively to the levels of $^2H_{11/2}$, $^4S_{3/2}$, and $^4F_{9/2}$, leading to the observation of the dominant green and red emissions by these transitions from the aforementioned states to the $^4I_{15/2}$ level.[40] As a benefit of the strong near-IR UC luminescence, the as-made $NaYF_4$:Yb,Er nanoparticles can be useful as building units for the rational design of optical probes for bio-imaging, singlet oxygen sensors for photodynamic therapy, colourful displays for document security, and photovoltaic cells for energy harvesting.[2]

Over the past decades, luminescent materials have been in the focus of intense research to develop their useful applications in electro-optical devices.[11, 12] Of particular interest is the class of luminescent materials, inorganic and organic components-emitting light, due to their unique physical features. The possibilities of practical applications of the luminescent materials are relevant to the concept of photo-durability and compatibility. Taking advantages over traditional fluorescences such as organic dyes, fluorescent proteins, and quantum dots, the near-IR responsive UC nanoparticles are an emerging class of luminescent nanomaterials with unique optical and physicochemical properties of high signal-to-noise ratio, superior photo-stability, long lifetimes, and lower photo-toxicity. As expected, the high photon UC efficiency leads to the as-made

$NaYF_4$:Yb,Er UC nanoparticles being attractive for rapid visualization of latent displays and security labels. The incorporation of the $NaYF_4$:Yb,Er UC nanoparticles into matrixes to obtain the resultant optical objects is currently attracting extensive interest to advance their potential uses in such technologies. To fabricate this type of the optical objects, we used the highly luminescent $NaYF_4$:Yb,Er nanoparticles composed of the major hexagonal β-phase and minor cubic α-phase as a UC guest for the fabrication of near-IR-sensitive components made of $NaYF_4$:Yb,Er particle-attached substrates and of $NaYF_4$:Yb,Er particle-assembled polymethyl methacrylate (PMMA) plastic membranes.

Latent tracks can be created by decorating the ethylene glycol-stabilized $NaYF_4$:Yb,Er nanoparticles on solid substrates. In a typical design, colloidal gels of the ethylene glycol-stabilized $NaYF_4$:Yb,Er nanoparticles were stamped on different substrates of lamellar wood, cloth fabric, and polystyrene plastic. We observed that the ethylene glycol-stabilized UC nanoparticles are attached tightly to the substrates to form a layer of coating after drying. Visibly, the substrates coated with the UC nanoparticles can emit easily and distinguishably strong green luminescence under 980 nm laser excitation (Figure 3f). This photo-luminescent feature could not be resolved clearly when viewing under ultraviolet and visible light. A two-photon laser-scanning luminescent micrograph (Figure 3g) of the tracks shows a fairly homogeneous distribution of distinct emitting domains of the UC nanoparticles bound to the substrate in comparison with no emission observed in the pristine substrate. The optical visualization of brilliant luminescence of the ethylene glycol-stabilized $NaYF_4$:Yb,Er nanocolloids solidified on the substrates offers the possibility to design latent fingermarks in authentication via molecular recognition-induced hybridization. It highlights that the advantages of photosensitivity, low-energy near-IR light, and low photo-toxicity in a solid-state material have inspired scientists to utilize the lanthanide-doped $NaYF_4$ nanoparticles for latent fingermark identification, additionally presenting safe operation of such technology in forensic science.[41, 42]

The distinct integration of highly near-IR-responsive UC nanoparticles into plastics makes the resultant functional composites useful for optical document security.[43-45] Strictly considering this potential utilization, we used PMMA as a polymeric matrix to co-assemble with the UC component to produce near-IR-emitting plastic films. The synthetic procedure is photo-induced polymerization of methyl methacrylate in a toluene dispersion containing oleic acid/ethylene glycol-stabilized $NaYF_4$:Yb,Er UC nanocolloids and 2,2-diethoxyacetophenone photo-initiator during evaporation-induced self-assembly to yield composite films. The resulting composites are crack-free, transparent, homogeneous plastics with a variable thickness, depending on the volume of the mixed solution employed in the assembly (Figures 4b,c). We found that the oleic acid/ethylene glycol-

stabilized UC nanoparticles are dispersible in the transparent PMMA matrix during polymerization for the assembly up to a particle loading concentration of ~0.15 g/g (15 wt%). This implies that the PMMA matrix also serves as a stabilizer to prevent the aggregation of the UC nanoparticles to result in recovering well-distributed composite membranes. We chose a moderate loading concentration of the oleic acid/ethylene glycol-stabilized $NaYF_4$:Yb,Er nanoparticles (~0.08 g/g, 8 wt%) in the PMMA matrix to investigate optical properties of the upconversion plastics.

The $NaYF_4$:Yb,Er/PMMA suspensions appear with intense green luminescence under 980 nm laser excitation (Figure 4a). After solvent evaporation and polymerization, the strong emission of the UC components appears uniformly in the composite films, suggesting a good distribution of the UC nanoparticles in the PMMA matrix. Unique features of UC photoluminescence spectroscopy and green emission of the $NaYF_4$:Yb,Er/PMMA composites resemble those of the pristine UC nanocolloids (Figures 4d–f). The magnitude of the emission intensity of the resulting composites scales with the UC particle concentration employed in the assembly. This indicates the conservation of surface properties of the $NaYF_4$:Yb,Er nanoparticles during PMMA polymerization. It is worth mentioning that the highly efficient multicolour UC luminescence of our composite plastics is comparable with that of lanthanide-doped $NaYF_4$/PMMA materials recently prepared by Yin et al.[46] and Boyer et at.[47] Conceptually, the distinct integration of low energy near-IR photons, transparency, and uniformity into the green-emitting polymeric membranes may allow designing them as an optical plastic for security seals to protect confidential documents.[48]

CONCLUSIONS

In summary, we have shown the distinct integration of upconversion luminescence of $NaYF_4$:Yb,Er nanocolloids into platforms to design near infrared optical components. The morphology and crystalline phase of $NaYF_4$:Yb,Er upconversion nanoparticles can be conducted upon hydrothermolysis of the reaction solution. The visible appearance of brilliant luminescence in both liquid and solid phases of the $NaYF_4$:Yb,Er nanocrystals can be a result of high photon upconversion efficiency. This unique optical feature makes the $NaYF_4$:Yb,Er upconversion nanomaterials attractive for investigating potential applications in biochemical sensing, biomedicine, and solar energy harvesting. One key implication of this present work is to use the as-made $NaYF_4$:Yb,Er nanocomponents as photon upconversion emitters to integrate into desired objects useful for advanced optical technologies. Upon solidification of the $NaYF_4$:Yb,Er nanocrystalline colloids into host matrices of substrates and polymethyl methacrylate plastics, the near infrared optical response of the upconversion components can be originally rendered in the resulting objects, paving a possible way for implementing fingerprint identification and labelling solutions for security and brand protection.

ACKNOWLEDGEMENTS

We are grateful to the National Foundation for Science and Technology Development of Vietnam under grant number 104.06-2014.87 for funding. HVD thanks to financial support from the Hue University Foundation Programme (DHH 2016-02-83).

REFERENCES

(1) C. Feldmann, T. Justel, C. R. Ronda, P. J. Schmidt, *Adv. Funct. Mater.* **2003**, *13*, 511.

(2) B. Zhou, B. Shi, D. Jin, X. Liu, *Nat. Nanotechnol.* **2015**, *10*, 924.

(3) H. A. Hoppe, *Angew. Chem. Int. Edit.* **2009**, *48*, 3572.

(4) T. M. Liu, J. Conde, T. Lipinski, A. Bednarkiewicz, C. C. Huang, *NPG Asia Materials* **2016**, *8*, DOI: 10.1038/am.2016.106.

(5) Y. A. Gromova, A. O. Orlova, V. G. Maslov, A. V. Fedorov, A. V. Baranov, *Nanoscale Res. Lett.* **2013**, *8*, 1.

(6) U. R. Genger, M. Grabolle, S. C. Jaricot, R. Nitschke, T. Nann, *Nat. Methods* **2008**, *5*, 763.

(7) O. K. Okamoto, L. Liu, D. L. Robertson, J. W. Hastings, *Biochemistry-US* **2001**, *40*, 15862.

(8) W. Park, D. Lu, S. Ahn, *Chem. Soc. Rev.* **2015**, *44*, 2940.

(9) F. Auzel, *Chem. Rev.* **2004**, *104*, 139.

(10) J. Zhao, D. Jin, E. P. Schartner, Y. Lu, Y. Liu, A. V. Zvyagin, L. Zhang, J. M. Dawes, P. Xi, J. A. Piper, E. M. Goldys, T. M. Monro, *Nat. Nanotechnol.* **2013**, *8*, 729.

(11) J. C. Goldschmidt, S. Fischer, *Advanced Optical Materials* **2015**, *3*, 510.

(12) J. Zhou, Q. Liu, W. Feng, Y. Sun, F. Li, *Chem. Rev.* **2015**, *115*, 395.

(13) D. Chen, Y. Chen, H. Lu, Z. Ji, *Inorg. Chem.* **2014**, *53*, 8638.

(14) G. Chen, H. Qiu, P. N. Prasad, X. Chen, *Chem. Rev.* **2014**, *114*, 5161.

(15) D. Chen, P. Huang, *Dalton T.* **2014**, *43*, 11299.

(16) M. Xu, D. Chen, P. Huang, Z. Wan, Y. Zhou, Z. Ji, *J. Mater. Chem.* **2016**, *4*, 6516.

(17) D. Chen, M. Xu, P. Huang, *Sensor. Actuat. B.Chem.* **2016**, *231*, 576.

(18) Z. Li, W. Park, G. Zorzetto, J. L. Summers, *Chem. Mater.* **2014**, *26*, 1770.

(19) Y. Wei, F. Lu, X. Zhang, D. Chen, *J. Alloy. Compd.* **2007**, *427*, 333.

(20) F. He, P. Yang, D. Wang, C. Li, N. Niu, *Langmuir* **2011**, *27*, 5616.

(21) C. Mi, Z. Tian, C. Cao, Z. Wang, C. Mao, S. Xu, *Langmuir* **2011**, *27*, 14632.

(22) X. Wang, J. Zhuang, Q. Peng, Y. Li, *Nature* **2005**, *437*, 121.

(23) F. Wang, R. Deng, X. Liu, *Nat. Protoc.* **2014**, *9*, 1634.

(24) X. Wang, X. Sun, D. Yu, B. Zou, Y. Li, *Adv. Mater.* **2003**, *15*, 1442.

(25) H. Mai, Y. Zhang, L. Sun, C. Yan, *J. Phys. Chem. C* **2007**, *111*, 13721.

(26) Z. Chen, L. Zhang, Y. Sun, J. Hu, D. Wang, *Adv. Funct. Mater.* **2009**, *19*, 3815.

(27) Y. I. Park, K. T. Lee, Y. D. Suh, T. Hyeon, *Chem. Soc. Rev*. **2014**, *44*, 1302.

(28) F. Zhang, Q. Shi, Y. Zhang, Y. Shi, K. Ding, D. Zhao, G. D. Stucky, *Adv. Mater.* **2011**, *23*, 3775.

(29) J. Wang, T. Wei, X. Li, B. Zhang, J. Wang, *Angew. Chem. Int. Edit.* **2014**, *53*, 1616.

(30) A. Baride, J. M. Meruga, C. Douma, D. Langerman, G. Crawford, J. J. Kellar, W. M. Cross P. S. May, *RSC Adv.* **2015**, *5*, 101338.

(31) M. You, J. Zhong, Y. Hong, Z. Duan, M. Lin, F. Xu, *Nanoscale* **2015**, *7*, 4423

(32) W. Xu, B. A. Bony, C. R. Kim, J. S. Baeck, Y. Chang, J. E. Bae, W. S. Chae, T. J. Kim, G. H. Lee, *Scientific Reports* **2013**, *3*, 3210.

(33) F. Zhang, T. Yu, F. Zhang, Y. Shi, S. Xie, Y. Li, L. Xu, B. Tu, D. Zhao, *Angew. Chem. Int. Edit.* **2007**, *119*, 8122.

(34) F. Wang, Y. Han, C. S. Lim, Y. Lu, J. Wang, J. Xu, H. Chen, C. Zhang, M. Hong, X. Liu, *Nature* **2010**, *463*, 1061.

(35) J. Guo, F. Ma, S. Gu, Y. Shi, J. Xie, *J. Alloy. Compd.* **2012**, *523*, 161.

(36) Q. Xuesong, P. Guohui, K. Y. Hyun, C. Yeqing, C. W. Jong, M. K. Byung, C. C. Byung, J. H. Jung, *Opt. Mater*. **2012**, *34*, 1007.

(37) H. H. Xie, Q. Wen, H. Huang, Q. Q. Wang, *RSC Adv.* **2015**, *5*, 79525.

(38) J. Zhao, Z. Lu, Y. Yin, C. McRae, J. A. Piper, J. M. Dawes, D. Jin, E. M. Goldys, *Nanoscale* **2013**, *5*, 944.

(39) X. Guo, C. Chen, D. Zhang, C. P. Tripp, S. Yin, W. Qin, *RSC Adv.* **2016**, *6*, 8127.

(40) H. Dong, L, D. Sun, C. H. Yan, *Nanoscale* **2013**, *5*, 5703.

(41) M. Wang, Y. Zhu, C. Mao, *Langmuir* **2015**, *31*, 7084.

(42) R. Ma, E. Bullock, P. Maynard, B. Reedy, R. Shimmon, C. Lennard, C. Roux, A. McDonagh, *Forensic Sci. Int*. **2011**, *207*, 145.

(43) A. J. Svagan, D. Busko, Y. Avlasevich, G. Glasser, S. Baluschev, K. Landfester, *ACS Nano* **2014**, *8*, 8198.

(44) X. Jiang, X. Guo, J. Peng, D. Zhao, Y. Ma, *ACS Appl. Mater. Interfaces* **2016**, *8*, 11441.

(45) C. Lin, M. T. Berry, R. Anderson, S. Smith, P. S. May, *Chem. Mater.* **2009**, *21*, 3406.

(46) Z. Yin, Y. Zhu, W. Xu, J, Wang, S. Xu, B. Dong, L. Xu, S. Zhang, H. Song, *Chem. Commun.* **2013**, *49*, 3781.

(47) J. C. Boyer, J. J. Johnson, F. C. J. M. Veggel, *Chem. Mater*. **2009**, *21*, 2010.

(48) T. C Mei, P. D. Swanand, R. E. Ricahard, *ACS Appl. Mater. Inter.* **2010**, *2*, 1884.

Figure Captions

Figure 1. (a) PXRD patterns and corresponding TEM images of the as-made samples of $NaYF_4$:Yb,Er UC nanocrystals hydrothermally prepared at 180 °C for 18 h in different reaction media: (b) ethanol, (c) ethanol-ethylene glycol, and (d) ethanol-ethylene glycol-oleic acid. (e) EDX spectrum of the samples prepared in ethanol-ethylene glycol, and (f) TGA curve (air, 10 °C·min^{-1}) of the samples prepared in ethanol-ethylene glycol-oleic acid.

Figure 2. PXRD patterns of $NaYF_4$:Yb,Er UC nanocrystal samples hydrothermally prepared in ethanol-ethylene glycol at different reaction temperatures (a) and times (b). TEM images of $NaYF_4$:Yb,Er UC nanocrystal samples hydrothermally prepared in ethanol-ethylene glycol at 180 °C for different reaction times: (c) 12 h, (d) 18 h, and (e) 36 h.

Figure 3. Photographs of ethylene glycol-stabilized $NaYF_4$:Yb,Er nanosphere colloids (a) before and (b) after solidification under 980 nm laser excitation show brilliant green luminescence. (c) Room-temperature UC luminescence spectra of $NaYF_4$:Yb,Er nanospheres hydrothermally prepared in ethanol-ethylene glycol at different reaction temperatures (160 °C - violet; 180 °C - blue; 200 °C - green) for 18 h under 980 nm laser excitation, inset shows a representative sample of the luminescent $NaYF_4$:Yb,Er nanocolloids. (d) Energy level diagram of photo-initiated energy transfer in a $NaYF_4$:Yb,Er upconversion nanocrystal, where Yb^{3+} sensitizer and Er^{3+} activator are co-doped in the $NaYF_4$ host. (e) UC luminescent lifetime decay curves of Er^{3+} dopant emission at 525.0 nm (left), 541.5 nm (middle), and 655.5 nm (right) for ethylene glycol-stabilized $NaYF_4$:Yb,Er nanosphere colloids. (f) Photographs of $NaYF_4$:Yb,Er nanosphere-stained substrates under 980 nm laser excitation. (g) Two-photon laser-scanning luminescent micrograph of ethylene glycol-stabilized $NaYF_4$:Yb,Er nanosphere-stained lamellar wood substrate under 980 nm laser excitation.

Figure 4. Near-IR light-emitting plastic films obtained from co-assembly of oleic acid/ethylene glycol-stabilized $NaYF_4$:Yb,Er UC nanocolloid guest with PMMA host. (a) Photograph of oleic acid/ethylene glycol-stabilized $NaYF_4$:Yb,Er/methyl methacrylate solution under 980 nm laser excitation. (b, c) Photographs of $NaYF_4$:Yb,Er/PMMA composite plastics obtained after photo-induced polymerization of the mixed solution. (d, e) Photographs of $NaYF_4$:Yb,Er/PMMA composite plastics under 980 nm laser excitation. (f) Room-temperature UC luminescence spectra of $NaYF_4$:Yb,Er/PMMA composite plastics under 980 nm laser excitation.

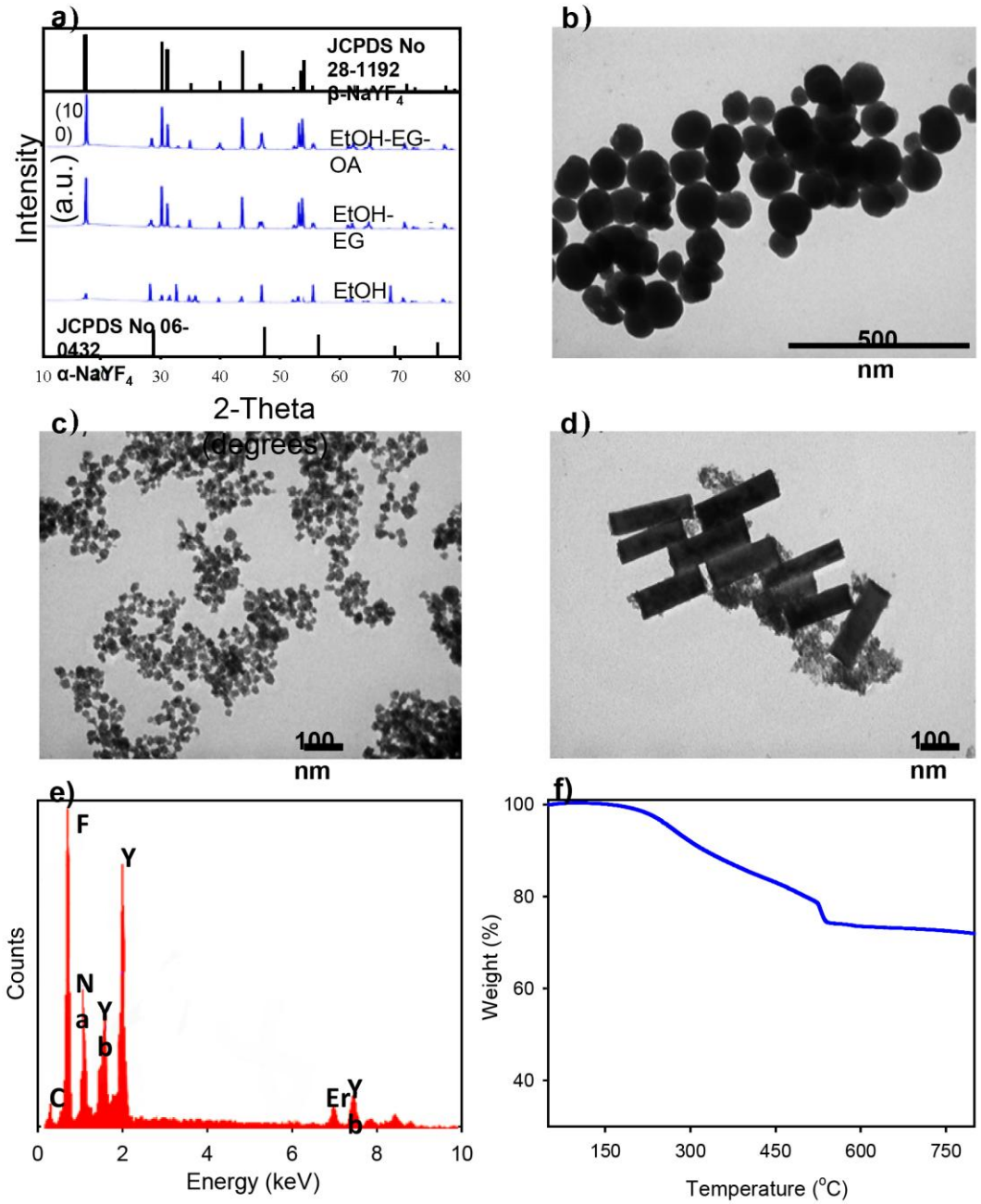

Figure 1

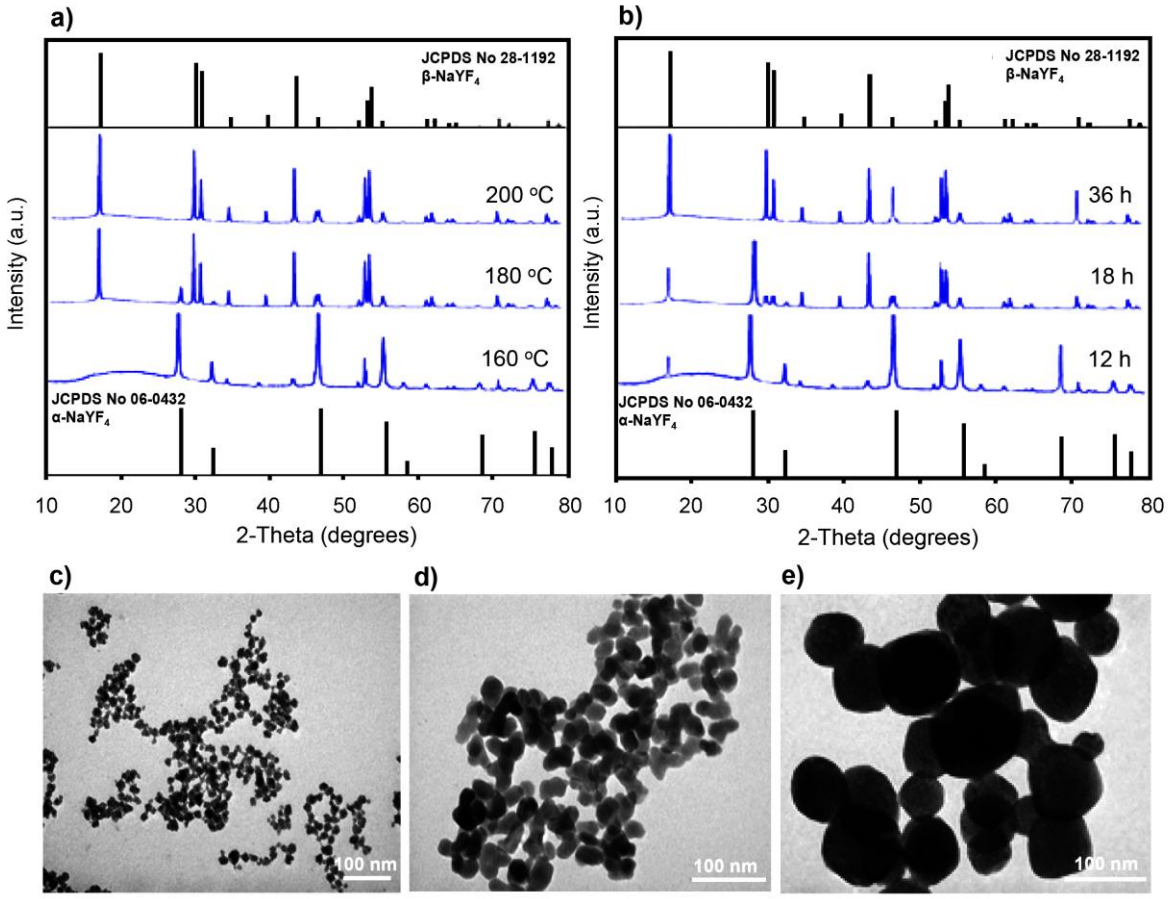

Figure 2

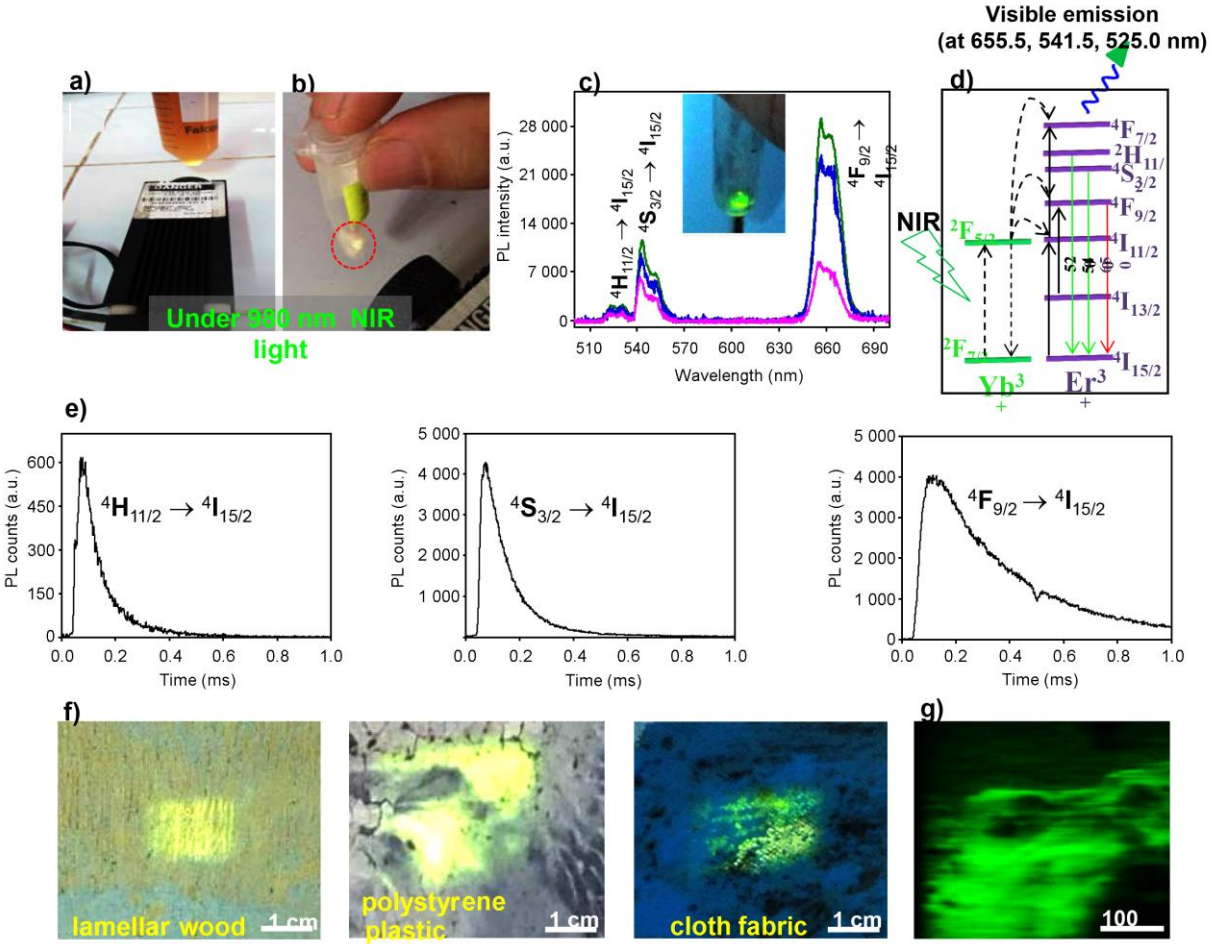

Figure 3

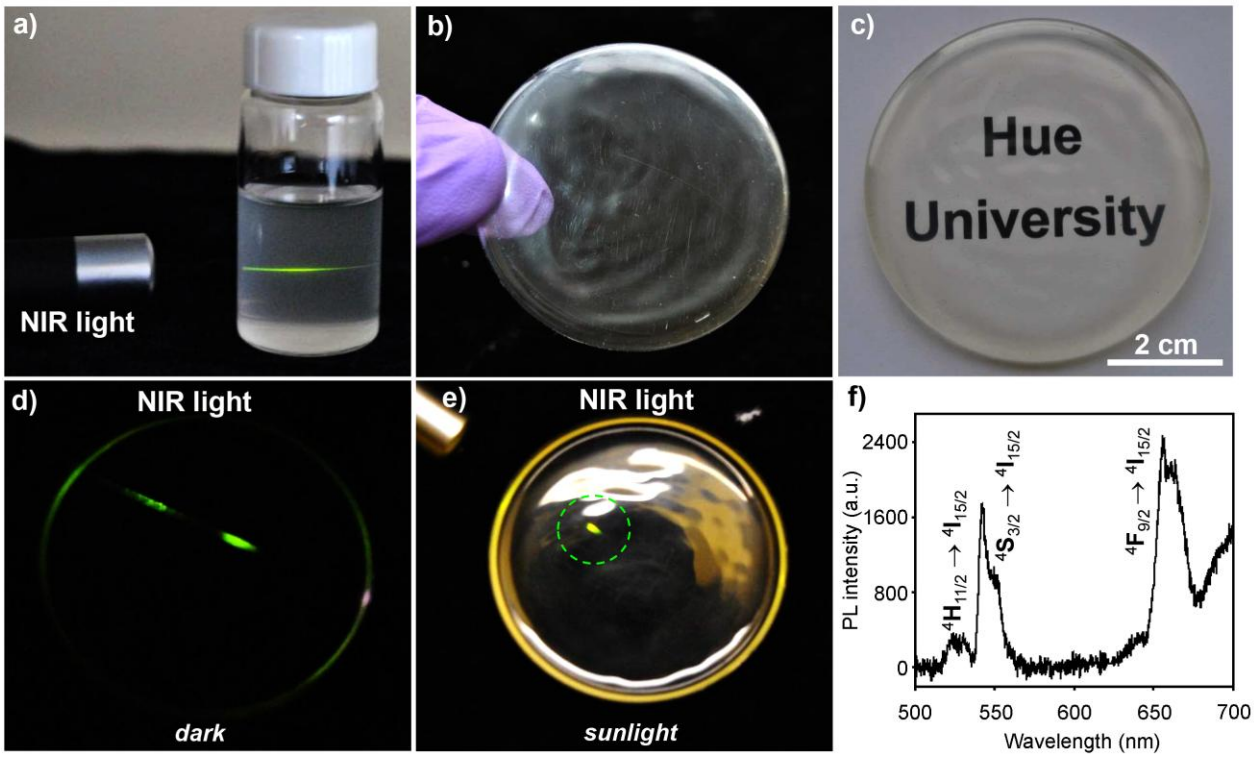

Figure 4